Dynamic Aspects in Host−Guest Interactions. 5. Kinetics of the Metal Complexation Reactions of 2-(5-Bromo-2-pyridylazo)-5-(*N*-propyl-*N*-sulfopropylamino)phenol Associated with Cyclodextrin Inclusion Reactions

Noboru Yoshida,*,† Hiroyuki Yamaguchi,‡ and Miwako Higashi§

Laboratory of Molecular Functional Chemistry, Division of Material Science, Graduate School of Environmental Earth Science, Hokkaido University, Sapporo 060, Japan, and Faculty of Engineering, Department of Materials Science, and Center for Cooperative Research and Development, Ibaraki University, Hitachi 316, Japan

Received: August 19, 1997; In Final Form: November 13, 1997

The kinetics of the 1:1 complex formation reactions of 2-(5-bromo-2-pyridylazo)-5-(*N*-propyl-*N*-sulfopropylamino)phenol (5-Br-PAPS) with some metal ions in the presence of α-, *β*-, and *γ*-cyclodextrin (α-, *β*-, and *γ*-CDx) have been investigated by the stopped-flow spectrophotometric method. The inclusion of 5-Br-PAPS by CDx causes a substantial decrease in the second-order formation rate constants owing to the steric hindrance to effective approach of metal ion to the specific orientation of 5-Br-PAPS in the CDx cavity and/or to the slower release of metal-coordinated water molecules in the apolar cavity. Binding of 5-Br-PAPS with cyclodextrins is indicated by change in the UV−vis absorption spectra and the ^{1}H NMR spectra. It is suggested that the reaction rates are governed by the presence of the encapsulated 5-Br-PAPS, which reacts more slowly with some metal ions in aqueous solution.

Introduction

It is well-established that the rate constants for the metal complex formation reactions in aqueous solution depend only slightly on the nature of the ligand and are characteristic of the rate-determining process for solvent exchange at metal centers in which a dissociative interchange (I_d) mechanism operates.[1] The outer-sphere association[2] (K_{os}) between metal ion and ligand is generally faster than rate-controlling solvent exchange (k_{M-H2O}) within the inner sphere. Therefore, the experimental forward rate constant, k_f, can be expressed by $fK_{os}k_{M-H2O}$, where f is the probability that the ligand will enter a particular coordination site.[3] However, the associative mechanism seems to be much more prevalent in such divalent and/or trivalent ions as Mn^{2+}, V^{2+}, and Fe^{3+}.[4] Effects of ionic charge, the internal conjugate base mechanism, and the ring-closure rate-determining step and steric effects are the crucial factors of the chelate ligands regulating the k_f value.[5] Retardation in the formation reaction rate due to macrocyclic effects and rate-limiting proton-transfer processes are also attributed exclusively to the steric and protonatable nature of the ligands.[5]

Furthermore, the k_f value also changes with the molecular environment in the vicinity of the ligand. Micellar[6] and solvent effects[7] on the rate and mechanism of the complex formation reactions are well-known. Micellar aggregates can solubilize the sparingly water-soluble ligands and compartmentalize various substrates, strongly modifying the chemical equilibria and reactivities. For example, the complexation of PADA (=pyridine-2-azo-*p*-dimethylaniline) with some transition-metal ions has been studied,[8] and the observed kinetic effects can be understood by theories such as the pseudo-phase separation model[9] and the electrostatic enrichment model at charged interfaces.[10]

The α-, *β*-, and *γ*-cyclodextrins are well-known to be most important and widely studied as host molecules that are capable of forming inclusion complex with a variety of guest molecules.[11] The catalytic effects of cyclodextrins on the organic reactions such as cleavage of esters have been studied extensively.[12] An ionized secondary hydroxy group of CDx in basic solution could form the covalent intermediate such as acylated CDx. On the other hand, CDx can simply provide an apolar and sterically restricted cavity for the included substrate, which can then serve as the microheterogenious reaction medium like a micelle.[11] While the catalytic effects on the kinetics of organic reactions have been so far extensively studied, relatively little attention has been paid to inorganic reactions. Recently, effects of CDx inclusion on the kinetics of the outer-sphere electron-transfer reaction have been reported.[13]

Recent research in our laboratory has been concerned with the kinetics of the inclusion reactions of some azo guest molecules such as 5-Br-PAPS with α-cyclodextrin. A directional multistep mechanism has been clearly observed in our series of kinetic studies.[14] The ligand 5-Br-PAPS has been known as highly sensitive photometric reagents for the zinc(II) ion.[15]

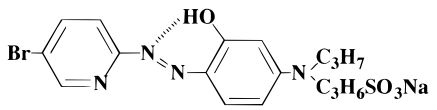

5-Br-PAPS

In this study, we have measured the formation rate of the metal−complex formation reactions of 5-Br-PAPS with some

† Hokkaido University.
‡ Department of Materials Science, Ibaraki University.
§ Center for Cooperative Research and Development, Ibaraki University.

S1089-5639(97)02686-8 CCC: $15.00
Published on Web 02/11/1998

TABLE 1: Rate Constants, k_f/mol^{-1} dm^3 s^{-1}, for 1:1 Chelate Formation of Some Bivalent Metal Ions in Aqueous Solution at 25 °C

	metal ions			
ligand	Co^{2+}	Ni^{2+}	Cu^{2+}	Zn^{2+}
5-Br-PAPS	4.3×10^4 [a]	5.50×10^2 [b]	1.10×10^6[b]	1.0×10^5 [b]
	2.95×10^4 [b]	7.6×10^2 [c]	2.1×10^6 [c]	
PADA	4×10^4(15 °C)	4×10^3	1×10^8(15 °C)	4×10^6(15 °C)
Bipy	6.3×10^4	1.6×10^3	4×10^7	1×10^6
Phen	3×10^5	3.9×10^3	6.4×10^7	1.1×10^6(15 °C)

[a] $I = 0.1$ mol dm^{-3} (NaCl) and $k_d = 8$ s^{-1}. [b] $I = 0.1$ mol dm^{-3} ($NaClO_4$) and $k_d = 2$ s^{-1} (Co^{2+}), 7×10^{-2} s^{-1} (Ni^{2+}), 20 s^{-1} (Cu^{2+}), and 2 s^{-1} (Zn^{2+}). [c] Haraguchi, K.; Ogata, T.; Nakagawa, K. *Mikrochim. Acta* **1992**, *106*, 75. As for PADA (pyridine-2-azo-*p*-dimethylaniline), Bipy (2,2′-bipyridine), and Phen (1,10-phenathroline), see ref 5.

bivalent metal ions in the presence of α-, *β*-, and *γ*-cyclodextrins. Binding constants of the inclusion complexes with α-, *β*-, and *γ*-CDx were independently determined by a UV−vis spectrophotometric method.

Experimental Section

Materials. 5-Br-PAPS was obtained from Dojindo. α-, *β*-, and *γ*-cyclodextrins were purchased from Tokyo Kasei Chemicals Co., Japan, and used without further purification. The water used in all the experiments was doubly distilled and deionized water. All other chemicals were reagent grade and used as received.

Measurements. Electronic absorption spectra were measured and the binding constants of the inclusion complexes of 5-Br-PAPS with CDx were determined spectrophotometrically using a JASCO V550 UV−vis spectrophotometer. The pH in solution was obtained using a Horiba pH meter D-13. The temperature was maintained at 25 ± 0.1 °C by means of an external circulating water bath (Thomas Kagaku Co. Ltd., TRL-108H). The circular dichroism (CD) spectra were measured with a JASCO J-600C circular dichrometer. The NMR spectra of the inclusion complexes were obtained at room temperature with a JEOL EX-400 FT NMR spectrometer (with TMS as an external reference). The kinetic measurements were performed by using a Unisoku optical-fiber type stopped-flow apparatus. Pseudo-first-order conditions of excess CDx and metal ion concentrations were maintained over 5-Br-PAPS. The observed rate constants (k_{obsd}) were determined from the average of three replicate experiments. The ionic strength was maintained at 0.1 mol dm^{-3} with $NaClO_4$ or NaCl.

Results and Discussion

Complex Formation in the Absence of CDx. *Reactions of Cobalt(II) Ion with 5-Br-PAPS.* The major form of 5-Br-PAPS is anionic LH^-, where H denotes the phenolic OH proton ($pK_a = 10.8$ determined by UV−vis spectroscopy). The observed rate constant (k_{obsd}) is related to k_f and k_d in eq 1 under a large excess of cobalt(II) ion and is expressed by eq 2.[16]

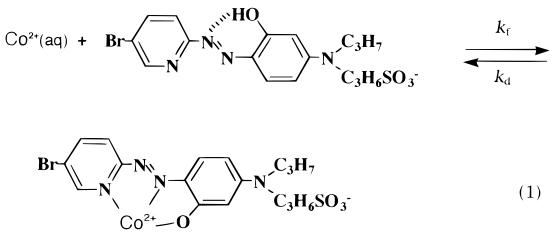

(1)

$$k_{obsd} = k_f[Co^{2+}] + k_d \qquad (2)$$

A plot of k_{obsd} against $[Co^{2+}]$ is linear, with slope k_f and intercept k_d at constant pH. The k_f value is slightly dependent on the pH region in the range 3.5−5.7 of the solution. The pK_a for propylamino proton H* was determined spectrophotometrically to be 5.90. Therefore, the following scheme is represented.

$$Co^{2+}(aq) + LHH^* \underset{k_{-1}}{\overset{k_1}{\rightleftharpoons}} CoLH^{*+} + H^+ \qquad (3)$$

$$Co^{2+}(aq) + LH^- \underset{k_{-2}}{\overset{k_2}{\rightleftharpoons}} CoL + H^+ \qquad (4)$$

In the lower pH region, only a small contribution of the LHH* species, where H* denotes the amino proton, would be considered. From the dependence of k_{obsd} versus $[H^+]$, the values of k_1 and k_2 were determined to be $(1.4 \pm 0.1) \times 10^4$ mol^{-1} dm^3 s^{-1} and $(2.8 \pm 0.1) \times 10^4$ mol^{-1} dm^3 s^{-1} at 25 °C and $I = 0.1$ mol dm^{-3} ($NaClO_4$). The activation parameters, $\Delta H_f^{\ddagger}$ and $\Delta S_f^{\ddagger}$ for the k_2 path, are also evaluated as 10.13 kcal mol^{-1} and − 9.74 cal K^{-1} mol^{-1}, respectively.

Reactions of Nickel(II), Copper(II), and Zinc(II) Ions with 5-Br-PAPS. The pH condition at ca. 5−7 is used in these reactions. The dependences of k_{obsd} versus $[M^{2+}]$ are the same as that for the Co^{2+}/5-Br-PAPS system. The rate constants for the complex formations are summarized in Table 1. The k_f values for Cu^{2+} and Zn^{2+} ions are lower by 1 order of magnitude than those for Cu^{2+}/bipy (log $k_f = 7$) and Zn^{2+}/bipy systems (log $k_f = 6.0$).[17]

Inclusion Stability. The stability constants for the α-, *β*-, and *γ*-CDx inclusion complexes with the LH^- form of 5-Br-PAPS were determined using UV−vis spectrophotometric titrations. Figure 1 shows the changes in the absorption spectra that occur when the LH^- form of 5-Br-PAPS binds to *β*-CDx.

The 1:1 inclusion model fits the titration data except for the *γ*-CDx/5-Br-PAPS system. A large decrease in absorbance (hypochromic effect) and a blue shift (448 nm → 442.5 nm) observed in the *γ*-CDx system suggest strongly the formation of the dimer species such as $(LH^-)_2$−*γ*CDx and/or $(LH^-)_2$−(*γ*-CDx)$_2$, which is induced within a larger *γ*-CDx cavity.[18,19] Figure 2 shows the differential absorption spectra in the *β*-CDx/5-Br-PAPS system.

The clear existence of several isosbestic points in Figure 2 would be related to the following simple 1:1 inclusion equilibrium.

$$LH^- + \beta\text{-CDx} \overset{K_f}{\rightleftharpoons} LH^- - \beta\text{CDx} \qquad (5)$$

The stability constant, K_f, was determined by the Hildebrand−Benesi analysis of the binding curves in Figure 3. The K_f values for the α-, *β*-, and *γ*- CDx inclusion complexes are determined to be 660, 510, and 1200 mol^{-1} dm^3, respectively. As for the *γ*-CDx system, K_f is only the parameter for the adjustment of

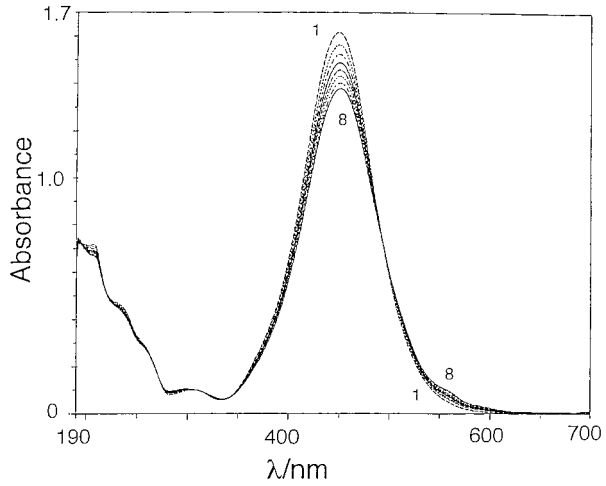

Figure 1. Spectral changes of 5-Br-PAPS at various β-CDx concentrations at pH = 6.8 and 25 °C: (1) 0, (2) 1.32 ([β-CDx]/[5-Br-PAPS] = 3.53), (3) 2.61 (7.06), (4) 3.88 (10.4), (5) 5.12 (13.7), (6) 6.34 (17.0), (7) 7.53 (20.1), (8) 8.70×10^{-4} mol dm^{-3} (23.3). [5-Br-PAPS] = 3.74×10^{-5} mol dm^{-3}.

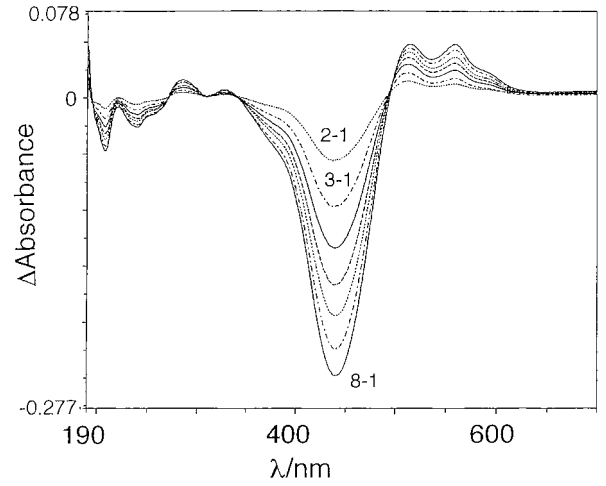

Figure 2. Differential absorption spectra between spectrum 1 and spectra 2−8 in Figure 1. Some clear isosbestic points are observed in the wider range of the concentration change of β-CDx.

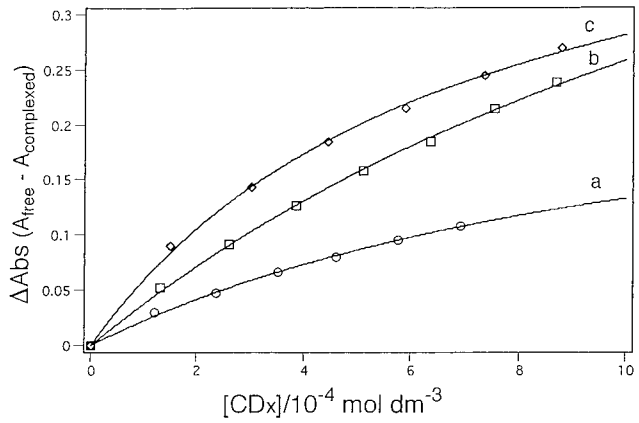

Figure 3. Binding curves for the 5-Br-PAPS inclusion complexes with α-CDx (a), β-CDx (b), and γ-CDx (c). [5-Br-PAPS] = 3.74×10^{-5} mol dm^{-3} at pH 6.8. The solid lines indicate the optimized theoretical curves to the observed data points.

the data to the Hildebrand−Benesi equation (vide infra). The final values of K_f by a nonlinear least-squares method (Damping Gauss−Newton method) are obtained as 850, 550, and 1400 mol^{-1} dm^3.

SCHEME 1

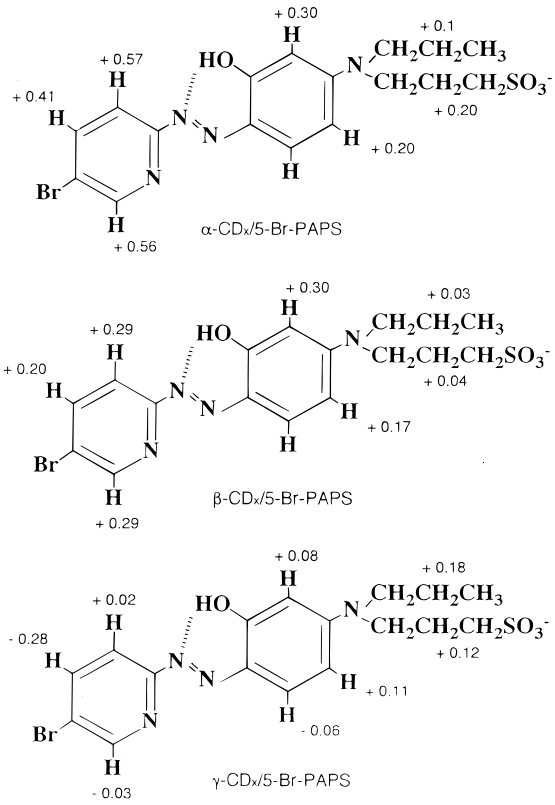

SCHEME 2

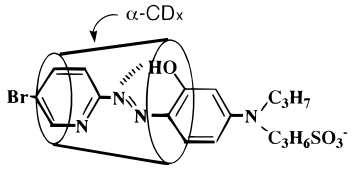

Representation of the encapsulated 5-Br-PAPS with α-CDx

Possible Structure of the Inclusion Complexes. Analysis by ^{1}H NMR of 5-Br-PAPS in the presence of α-, β-, and γ-CDx in D_2O gave results quantitatively similar to those obtained in the inclusion complexes of an analogous azo guest molecule.[20] Since the chemical exchange for the inclusion of 5-Br-PAPS by CDx is rapid compared with the NMR time scale, only one set of concentration-dependent resonances are observed. The values of chemical shifts in Scheme 1 are those for the fully encapsulated 5-Br-PAPS by CDx. Larger downfield shifts were observed for the ring protons of bromopyridine, clearly indicating the formation of the regioselective inclusion complex in D_2O (Scheme 1, the symbol "+" shows the downfield shift and "−" the upfield shift).

In the α-CDx inclusion system, it was inferred that significant downfield shifts of the bromopyridene protons imply the selective interaction of this moiety with α-CDx. From the CPK molecular model consideration, it was shown that the inclusion of 5-Br-PAPS from the *N*-propyl-*N*-sulfopropylphenol moiety is completely blocked due to the larger steric hindrance (Scheme 2).[14b] This selective inclusion is not observed in the β-CDx/5-Br-PAPS system (Scheme 1) because of the larger cavity of β-CDx, which results in the lack of tight and selective size-compatible fit for recognition. Upon the γ-CDx/5-Br-PAPS complex formation, only small downfield shifts and slight upfield shifts were observed, as shown in Scheme 1, and would

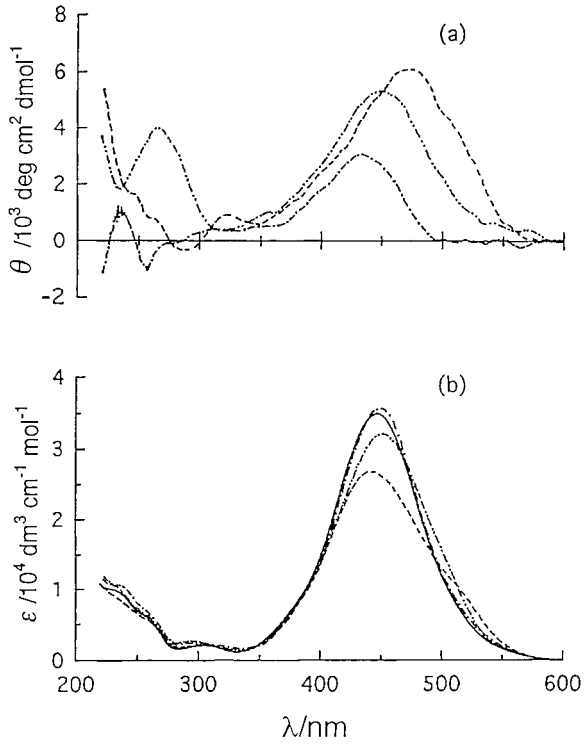

Figure 4. Induced circular dichroism (top) and absorption (bottom) spectra of the α- (-•), *β*- (-••-), and *γ*-cyclodextrin (- - -) complexes of 5-Br-PAPS at pH = 7 and 25 °C. [α-CDx] = [*β*-CDx] = [*γ*-CDx] = 1.0×10^{-2} mol dm^{-3}. [5-Br-PAPS] = 2.95×10^{-5} mol dm^{-3}. Solid line denotes the absorption spectrum of 5-Br-PAPS only.

SCHEME 3

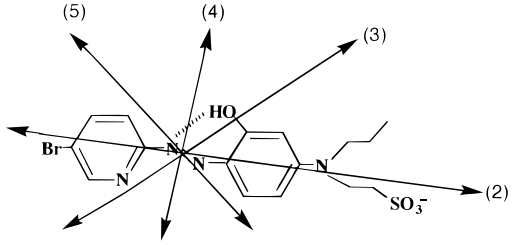

be attributed to mutual ring current effects by the dimerization of 5-Br-PAPS in the *γ*-CDx cavity.[19]

The induced circular dichroism (ICD) spectra were observed on the absorption bands of the achiral 5-Br-PAPS, which is included in the assymmetric field of the cyclodextrin cavity (Figure 4). The $\pi-\pi^*$ electronic transition at 447 nm, which is polarized along the long axis of 5-Br-PAPS from the calculation by the ZINDO method (Scheme 3 and Table 2), shows almost a single positive ICD in the α-CDx inclusion complex. This result indicates that the direction of the electronic dipole moment in the chromophore is almost parallel to the long axis of the α-CDx cavity.[19] The ICD spectrum of *β*-CDx/5-Br-PAPS is somewhat different from that of α-CDx/5-Br-PAPS, particularly in the UV region at ca. 265 nm, indicating the different structural features such as the orientation of the chromophore within the CDx cavity.

In general, the weaker effect of *γ*-CDx upon the strength of the ICD spectrum is observed because of the lack of a tight and size-compatible fit for recognition as compared with the effect of α- and *β*-CDx. However, the relatively strong ICD strength and the appearance of a shoulder band above 500 nm are observed, as shown in Figure 4. This characteristic ICD pattern would be related with the dimerization of the chromophore. The representative split-type ICD spectrum, which is often observed because of the dimerization of chromophores within the *γ*-CDx cavity,[19] is not observed in this *γ*-CDx/5-Br-PAPS. We are not able to explain this spectral pattern at the moment.

TABLE 2: Experimental $\pi-\pi^*$ Transition Energies and Extinction Coefficents (ϵ) and Calculated Results of Transition Energies (λ_{max}/nm) and Oscillator Strengths (*f*) of 5-Br-PAPS by the ZINDO[a] Method

	experimental		calculation		
band	λ_{max}	ϵ	λ_{max}	*f*	polarization[b]
1			518	0.000	(*n*N=N → π^*)
2	447	35 000	387	1.047	−10
3			318	0.024	25
4			283	0.015	70
5	304	2060	266	0.129	−70
6			260	0.007	90[c]
7			248	0.088	86

[a] Ridley, J.; Zerner, M. C. *Theor. Chim. Acta* **1973**, *32*, 111. Anderson, W. P.; Edwards, W. D.; Zerner, M. C. *Inorg. Chem.* **1986**, *25*, 2728. [b] The angle of the transition moment to the *x*-axis (long axis). [c] (*z*-axis) ($\pi \rightarrow \sigma^*$).

Complex Formation Kinetics in the Presence of CDx. The rate constants for the metal complex formation were found to decrease as the concentration of added cyclodextrin was increased. Figure 5 shows the plots of k_{obsd} against [Co^{2+}] for the metal complex formation of 5-Br-PAPS in the absence and in the presence of *β*-CDx. Decreases in the slope (k_f) and the intercept (k_d) were observed. Plots of k_f versus [CDx] in the α-, *β*-, and *γ*-CDx systems are shown in Figure 6.

The values of k_f decrease with an increase of [CDx] and at a higher CDx concentration show a saturated behavior. These concentration dependences of k_f versus [CDx] could be interpreted in terms of the mechanism shown in Scheme 4.

SCHEME 4

$$LH^- + CDx \overset{K_f}{\rightleftharpoons} LH^- - CDx$$

$$LH^- + Co^{2+}(aq) \xrightarrow{k_{un}} CoL + H^+$$

$$LH-CDx^- + Co^{2+}(aq) \xrightarrow{k_{CDx}} CoL-CDx + H^+$$

From this reaction mechanism, the rate law may be written as follows.

$$d[L-Co^{2+}]_T/dt = k_f[Co_{aq}^{2+}]_T[L] \qquad (6)$$

where

$$k_f = \frac{k_{CDx} - k_{un}}{1 + (K_f[CDx])^{-1}} + k_{un}$$

$$= \frac{k_{un} + k_{CDx}K_f[CDx]}{1 + K_f[CDx]} \qquad (7)$$

If k_{un} is larger than $k_{CDx}K_f[CDx]$, k_f^{-1} would be equal to $k_{un}^{-1} + K_f[CDx]/k_{un}$. In most cases, the plot of k_f^{-1} versus [CDx] gives a linear relation with a slope K_f/k_{un} and an intercept k_{un}^{-1}. The values of $K_{f,CDx}$, k_{un}, and k_{CDx} are summarized in Table 3.

Two possibilities for the decrease in the rate constants k_f in the presence of CDx could be considered: (1) steric hindrance of metal ions to the specific orientation of 5-Br-PAPS in the

TABLE 3: Binding Constants, K_f, for the Inclusion Reactions and Rate Constants, k_{un} and k_{CDx}, for the Metal Complexation Reactions of 5-Br-PAPS in the Absence and Presence of Cyclodextrins

	metal ions			
	Co^{2+}	Ni^{2+}	Cu^{2+}	Zn^{2+}
$K_{f,\alpha-CDx}$/mol^{-1} dm^3	$(6.5 \pm 0.6) \times 10^2$	$(6.5 \pm 0.2) \times 10^2$	$(7.0 \pm 0.2) \times 10^2$	
	6.7×10^2	6.5×10^2	7.0×10^2	
$K_{f,\beta-CDx}$/mol^{-1} dm^3	$(8.2 \pm 1.2) \times 10^2$	$(7.0 \pm 1.2) \times 10^2$	$(4.9 \pm 2.2) \times 10^2$	
	5.5×10^2	6.0×10^2	4.9×10^2	
$K(_{\gamma-CDx})$[a]	$(1.1 \pm 0.2) \times 10^3$	$(1.8 \pm 0.5) \times 10^2$	$(2.0 \pm 0.4) \times 10^2$	
	1.2×10^3	2.0×10^2	1.8×10^2	
k_{un}/mol^{-1} dm^3 s^{-1}	(4.30×10^4)[b]	5.5×10^2	1.1×10^6	1.1×10^5
	(2.95×10^4)[c]			
$k_{\alpha-CDx}$/mol^{-1} dm^3 s^{-1}	$(8.9 \pm 0.8) \times 10^2$	15 ± 0.1	$(4.3 \pm 0.3) \times 10^5$	*d*
$k_{\beta-CDx}$/mol^{-1} dm^3 s^{-1}	$(2.7 \pm 0.1) \times 10^3$	30 ± 0.3	$(1.1 \pm 0.4) \times 10^5$	*d*
$k(_{\gamma-CDx})$[a]	$(2.3 \pm 0.7) \times 10^3$	30 ± 0.1	$(2.0 \pm 0.1) \times 10^5$	

[a] $K(_{\gamma-CDx})$ and $k(_{\gamma-CDx})$ are the parameters for the adjustment of the data to eq 6. No physical meaning is obtained. [b] Since ClO_4^- ion forms a relatively stable inclusion complex with α-CDx, the ionic strength was adjusted using NaCl at 0.1 mol dm^{-3}. [c] $I = 0.1$ mol dm^{-3} ($NaClO_4$). [d] The change in visible absorption spectrum proceeds clearly in two steps. Effect on the rate constant, k_f, is negligible. However, the dissociation of the Zn^{2+} complex appears to be completely inhibited. The value of k_d approaches zero upon increasing [CDx]. The values K_f in the second column were calculated from the plot of k_f^{-1} vs [CDx].

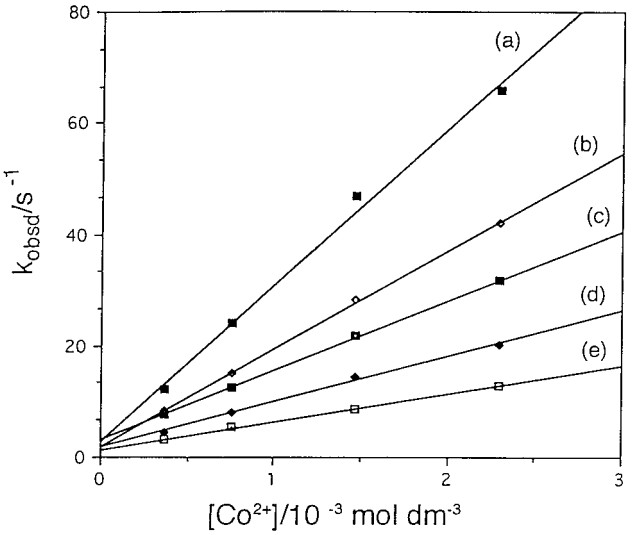

Figure 5. Plots of k_{obsd} against [Co^{2+}] for the cobalt(II) complex formation of 5-Br-PAPS in the presence of β-cyclodextrin: (a) 0, (b) 1, (c) 2, (d) 5, (e) 10×10^{-3} mol dm^{-3}. [5-Br-PAPS] $= 3.5 \times 10^{-6}$ mol dm^{-3}. pH = 5.7.

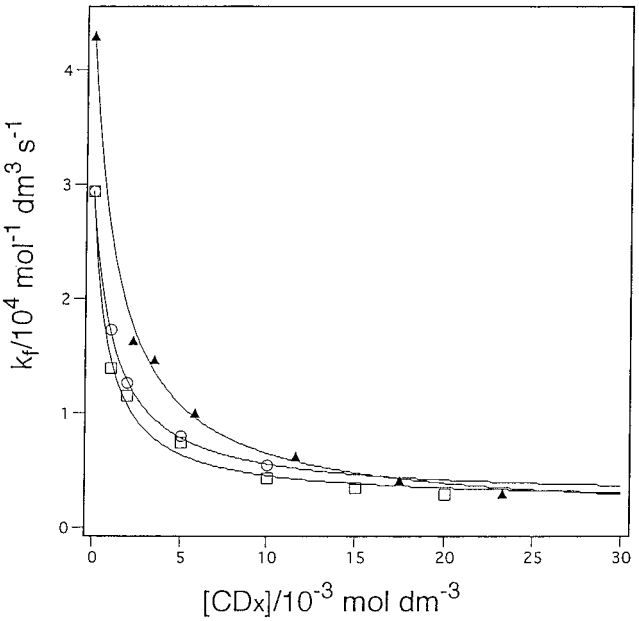

Figure 6. Dependences of the second-order formation rate constants, k_f, on [CDx] for the cobalt complex formation reaction in the presence of α-CDx (▲), β-CDx (○), and γ-CDx (□). Solid lines show the theoretical curves by a nonlinear least-squares method. The theoretical values for k_f and K_{CDx} are obtained from these curves and are summarized in Table 3.

CDx cavity and (2) the slower release of metal-coordinated water molecules in the apolar CDx cavity. The inner diameters of the CDx cavity were 4.2−8.8 Å for α-CDx, 5.7−10.8 Å for β-CDx, and 6.8−12.0 Å for γ-CDx, while the depth of the binding cavity of all three cyclodextrins is about the same (7.8 Å).[21] The length of 5-Br-PAPS along the long axis is about 21 Å. In the α-CDx system, the bromopyridine moiety of 5-Br-PAPS is tightly encapsulated and the *N*-propyl-*N*-sulfopropyl-aminophenol site is positioned outside of the CDx cavity. Therefore, the approach of the metal ion to the coordination site is strictly hindered. The substantial decrease of k_f in the presence of α-CDx ($k_{\alpha-CDx}/k_{un} = 1/48$ for Co^{2+} and 1/37 for Ni^{2+}) would be mainly attributable to this steric origin. The relatively small effects on the k_f value found in β-CDx ($k_{\beta-CDx}/k_{un} = 1/11$ for Co^{2+} and 1/18 for Ni^{2+}) and γ-CDx ($k_{\gamma-CDx}/k_{un} = 1/13$ for Co^{2+} and 1/18 for Ni^{2+}) systems are due to the lack of a size-compatible fit for recognition as compared with the effect of α-CDx.[19] The metal ions such as Co^{2+} and Ni^{2+} could be accesible to the loosely encapsulated 5-Br-PAPS with β-CDx and γ-CDx. In this case, the slower release of the metal-coordinated water molecules may occur in the apolar CDx cavity.

A smaller effect of k_f on the cyclodextrin concentration was observed in the Cu^{2+} complex formation reaction with 5-Br-PAPS ($k_{\alpha-CDx}/k_{un} = 1/2.6$, $k_{\beta-CDx}/k_{un} = 1/10$, and $k_{\gamma-CDx}/k_{un} = 1/5$). The clarification of this unexpected smaller dependence of k_f upon the cyclodextrin concentration is now in progress using other ligand systems.

Figure 7 shows the rapid-scan spectra of the formation of the Zn^{2+} complex of 5-Br-PAPS in aqueous solution, indicating the presence of the isosbestic point and the one-step formation kinetics. However, in the presence of CDx, the Zn^{2+} complex formation of 5-Br-PAPS proceeds clearly in two steps (fast and slow steps in Figure 8). The pyridyl-*o*-phenolic ligand such as 5-Br-PAPS is markedly different from the other ligands such as bipy and phen. An intramolecular hydrogen bond can form between the *o*-OH group and a nitrogen atom (Scheme 5).[22]

The existence of the OH···N type intramolecular hydrogen bond may lead to the two-step mechanism as shown in Scheme 4.[23] The detection of the *N*,*N*-bidentate intermediate species

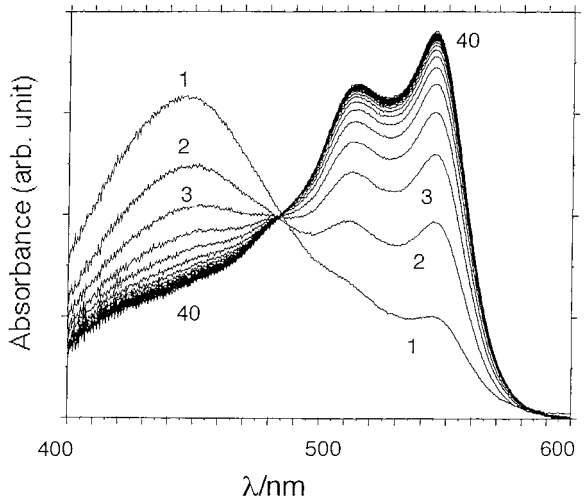

Figure 7. Time-dependent spectra of the Zn^{2+} complex formation reaction of 5-Br-PAPS in aqueous solution at 25 °C. [5-Br-PAPS] = 3.5×10^{-6} mol dm^{-3} and [Zn^{2+}] = 1.4×10^{-4} mol dm^{-3} (gate time per spectrum = 10 ms and total rapid-scan time = 1.17 s for spectrum 40).

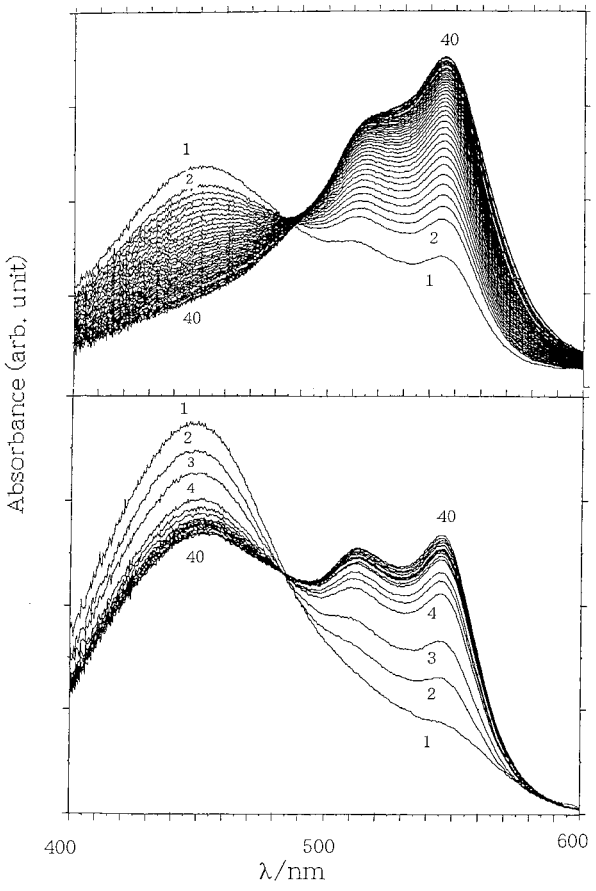

Figure 8. Time-dependent spectra for the fast step (bottom) and the slow step (top) of the Zn^{2+} complex formation reaction of 5-Br-PAPS in the presence of α-cyclodextrin at 25 °C. [α-CDx] = 1.0×10^{-2} mol dm^{-3}. [5-Br-PAPS] = 3.5×10^{-6} mol dm^{-3} and [Zn^{2+}] = 1.4×10^{-4} mol dm^{-3} (gate time per spectrum = 10 ms and total rapid-scan time = 1.17 s for the fast step and gate time per spectrum = 500 ms and total rapid-scan time = 234 s for the slow step).

has been already carried out by our group.[23c] The *N*,*N*-bidentate species is confirmed only in apolar solvent such as dioxane and is fragile even to the moisture in air. Since the polarity of CDx is assumed to be that of dioxane ($\epsilon = 2.2$),[24] the two-step change

SCHEME 5

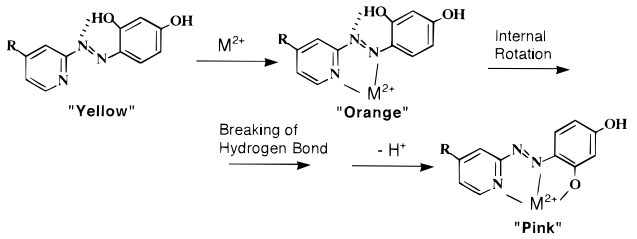

in the visible absorption spectrum in Figure 8 would be related closely to the two-step mechanism shown in Scheme 5.

The formation of the tridentate complex requires the rupture of the internal OH···N hydrogen bond, the rotation of the *N*-propyl-*N*-sulfopropylaminophenol ring, and the deprotonation of the *o*-OH group. The formation of the *N*,*N*-bidentate species causes a much smaller absorption change than that of the *N*,*N*,*O*-tridentate complex which requires the *o*-OH deprotonation.[23c] The final ring-closure step may be retarded in the apolar size-restricted CDx cavity. This kinetic effect of CDx is specific only in the Zn^{2+} complex formation.

Supporting Information Available: Table of kinetic data on the Co^{2+} complexation with 5-Br-PAPS (3 pages). Ordering information is given on any current masthead page.

References and Notes

(1) R. Wilkins, G. *Acc. Chem. Res* **1970**, *3*, 408. Langford, C. H. *Ionic Interactions*; Petrucci, S., Ed.; Academic Press: New York, 1971. Wilkins, R. G. *The Study of Kinetics and Mechanism of Reactions of Transition Metal Complexes*; Allyn and Bacon: Boston, 1974. Jordan, R. B. *Reaction Mechanisms of Inorganic and Organometallic Systems*; Oxford University Press: Oxford, 1991.

(2) Fuoss, R. M. *J. Am. Chem. Soc.* **1958**, *80*, 5059. Eigen, M. *Z. Elektrochem.* **1960**, *64*, 115. Prue, J. E. *J. Chem. Soc.* **1965**, 7534.

(3) Neely, J.; Connick, R. *J. Am. Chem. Soc.* **1970**, *92*, 3476.

(4) Merbach, A. E. *Pure Appl. Chem.* **1982**, *54*, 1479.

(5) Margerum, D. W.; Cayley, G. R.; Weatherburn, D. C.; Pagenkopf, G. K. *Coordination Chemistry Vol. 2*; Martell, A. E., Ed.; American Chemical Society: Washington, DC, 1978.

(6) Carbone, A. I.; Cavasino, F. P.; Sbriziolo, C. *J. Phys. Chem.* **1987**, *91*, 4062. Fletcher, P. D. I.; Robinson, B. H. *J. Chem. Soc., Faraday Trans, 1* **1984**, *80*, 2417. Tachiyashiki, S.; Yamatera, H. *Inorg. Chem.* **1986**, *25*, 3043. Ige, J.; Soriyan, O. *J. Chem. Soc., Faraday Trans. 1* **1986**, *82*, 2011. Dash, A. C.; Nayak, R. C. *J. Chem. Soc., Faraday Trans. 1* **1987**, *83*, 1307. Cavasino, F. P.; Sbriziolo, C.; Pelizzetti, E.; Pramauro, E. *J. Phys. Chem.* **1989**, *93*, 469.

(7) Caldin, E. F.; Bennetto, H. P. *J. Solution Chem.* **1973**, *2*, 217. Burgess, J.; Twigg, M. V. *J. Chem. Soc., Dalton Trans.* **1974**, 2032. Buck, D. M. W.; Moore, P. *J. Chem. Soc., Dalton Trans.* **1975**, 409. Chattopadhyay, P. K.; Coetzee, J. F. *Anal. Chem.* **1974**, *46*, 2014. Mackellar, W. J.; Rorabacher, D. B. *J. Am. Chem. Soc.* **1971**, *93*, 4379. Mentasti, E.; Baiocchi, C.; Kirschenbaum, L. J. *J. Chem. Soc., Dalton Trans.* **1985**, 2615.

(8) Calvaruso, G.; Cavasino, F. P.; Di Dio, E. *Inorg. Chim. Acta* **1986**, *119*, 29 and references therein.

(9) Berezin, I. V.; Martinek, K.; Yatsmirsckii, A. *Russ. Chem. Rev. (Engl. Transl.)* **1973**, *42*, 787. Fendler, J. H.; Fendler, E. J. *Catalysis in Micellar and Macromolecular Systems*; Academic Press: New York, 1975. Romsted, L. S. *Surfactants in Solutions*; Mittal, K. L., Lindman, B., Eds.; Plenum: New York, 1984.

(10) Diekmann, S.; Frahm, J. *J. Chem. Soc., Faraday Trans. 1* **1979**, *75*, 2199; **1980**, *76*, 446. Chevalier, Y.; Chachaty, C. *J. Am. Chem. Soc.* **1985**, *107*, 1102.

(11) Bender, M. L.; Komiyama, M. *Cyclodextrin Chemistry*; Springer Verlag: New York, 1978. Saenger, W. *Angew. Chem., Int. Ed. Engl.* **1980**, *19*, 344. Szejtli, J. *Cyclodextrim and their Inclusion Complexes*; Akademiai Kiado: Budapest, 1982. G. Wenz, *Angew. Chem. Int. Ed. Engl.* **1994**, *33*, 803.

(12) Gadosy, T. A.; Tee, O. S. *J. Chem. Soc., Perkin Trans. 2*. **1995**, 71 and reference therein.

(13) Johnson, M. D.; Reinsborough, V. C.; Ward, S. *Inorg. Chem.* **1992**, *31*, 1085. Imonigie, J. A.; Macartney, D. H. *Inorg. Chem.* **1993**, *32*, 1007.

(14) (a) Yoshida, N.; Fujimoto, M. *J. Phys. Chem*. **1990**, *94*, 4246. (b) Yoshida, N.; Hayashi, K. *J. Chem. Soc., Perkin Trans. 2*. **1994**, 1285. (c) Yoshida, N.; Fujita, Y. *J. Phys. Chem*., **1995**, *99*, 3671. (d) Yoshida, N.; *J. Chem. Soc., Perkin Trans. 2*., **1995**, 2249.

(15) Makino, T.; Saito, M.; Horiguchi, D.; Kina, K. *Clin. Chim. Acta* **1982**, *120*, 127. Horiguchi, D.; Saito, M.; Noda, K.; Kina, K. *Anal. Sci*. **1985**, *1*, 461.

(16) The slow reaction due to the oxidation of Co(II) center was observed.

(17) Holyer, R. H.; Hubbard, C. D.; Kettle, S. F. A.; Wilkins, R. G. *Inorg. Chem*. **1965**, *4*, 929; **1966**, *5*, 622.

(18) Clarke, R. J.; Coates, J. H.; Lincoln, S. F. *J. Chem. Soc., Faraday Trans. 1* **1984**, 3119.

(19) Yoshida, N.; Yamaguchi, H.; Higashi, M. *J. Chem. Soc., Perkin Trans 2* **1994**, 2507.

(20) Yoshida, N.; Fujimoto, M. *Bull. Chem. Soc. Jpn*. **1982**, *55*, 1039.

(21) Garces, F. O.; Rao, V. P.; Garibay, M. A. G.; Turro, N. J. *Supramol. Chem*. **1992**, *1*, 65.

(22) Yoshida, N.; Fujimoto, M. *Bull. Chem. Soc. Jpn*. **1976**, *49*, 1557.

(23) (a) Hubbard, C. D.; Pacheco, D. *J. Inorg. Nucl. Chem*. **1977**, *39*, 1373. (b) Reeves, R. L.; Calabrese, G. S.; Harkway, S. A. *Inorg. Chem*. **1983**, *22*, 3076. (c) Kudo, Y.; Yoshida, N.; Imamura, T.; Fujimoto, M. *Bull. Chem. Soc. Jpn*. **1984**, *57*, 3099.

(24) VanEtten, R. L.; Sebastian, J. F.; Clowes, G. A.; Bender, M. L. *J. Am. Chem. Soc*. **1967**, *89*, 3242.